



The following Communications have been judged by at least two referees to be “very important papers” and will be published online at www.angewandte.org soon:

Q. Zhang, T. P. Chou, B. Russo, S. A. Jenekhe, G. Cao*
Aggregation of ZnO Nanocrystallites for High Conversion Efficiency in Dye-Sensitized Solar Cells

S. Arita, T. Koike, Y. Kayaki, T. Ikariya*
Aerobic Oxidative Kinetic Resolution of Racemic Secondary Alcohols with Chiral Bifunctional Amido Complexes

C. Ruspic, J. R. Moss, M. Schürmann, S. Harder*
Remarkable Stability of Metallocenes with Superbulky Ligands: Spontaneous Reduction of Sm^{III} to Sm^{II}

T. A. Rokob, A. Hamza, A. Stirling, T. Soós,* I. Pápai*
Turning Frustration into Bond Activation: A Theoretical Mechanistic Study on Heterolytic Hydrogen Splitting by Frustrated Lewis Pairs

L. M. Fidalgo, G. Whyte, D. Bratton, C. F. Kaminski, C. Abell, W. T. S. Huck*

From Microdroplets to Microfluidics: Selective Emulsion Separation in Microfluidic Devices

News

New Members of the International Advisory Board: G. R. Desiraju, D. Gatteschi, K. Kim, S. G. Withers

2728

Books

Modern Alkaloids

Ernesto Fattorusso,
 Orazio Tagliatella-Scafati

reviewed by P. Spiteller 2730

Name Reactions for Functional Group Transformations

Jie Jack Li

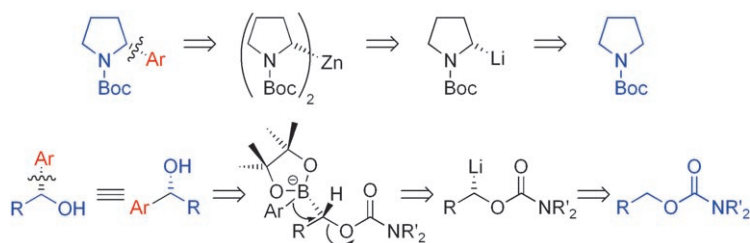
reviewed by D. Sälinger 2731

Highlights

Carbanion Arylations

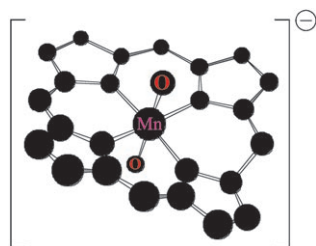
P. O'Brien,* J. L. Bilke 2734–2736

Expanding the Synthetic Potential of Asymmetric Deprotonation: Arylation of Carbanions



Aryl unplugged: Two conceptually new disconnections are equivalent to arylation of enantioenriched carbanions obtained by asymmetric deprotonation. One retrosynthesis (see scheme, above) involves *N*-

Boc pyrrolidine (Boc = *tert*-butoxycarbonyl, Ar = aryl) and an organozinc intermediate, and the other (below) *O*-alkyl carbamates with organoboron intermediates.



Double O agents: The first definitive spectroscopic evidence for *trans*-dioxomanganese(V) porphyrins (see picture) has been reported by Groves, Spiro, and co-workers. Their work extends the scope of oxo-coordination chemistry and opens the way for the exploration of reactivity patterns of *trans*-dioxo complexes of first-row transition-metal ions.

Dioxo Complexes

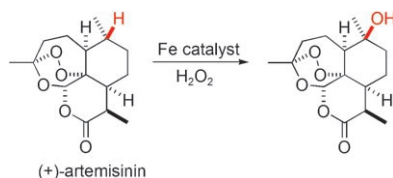
Z. Gross* 2737–2739

The Groves–Spiro Dioxomanganese(V) Story

C–H Activation

M. Christmann* _____ 2740–2742

Selective Oxidation of Aliphatic C–H Bonds in the Synthesis of Complex Molecules



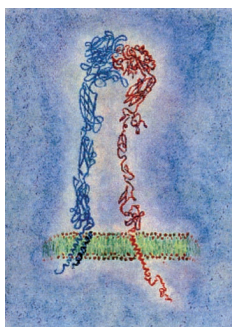
Tamed cat: Iron-catalyzed selective C–H oxidation reactions present new possibilities in the synthesis and modification of natural products. As a model reaction of a possible C–H oxidation as part of a total synthesis, the natural product (+)-artemisinin was converted into (+)-10β-hydroxyartemisinin in 34% yield (see scheme). The combination of nontoxic metal catalyst with H₂O₂ is an environmentally friendly process.

Minireviews

Membrane Proteins

H. Yin* _____ 2744–2752

Exogenous Agents that Target Transmembrane Domains of Proteins



Over the limit: Despite accounting for about one third of all proteins encoded in the human genome, the functions and structures of the transmembrane domains of membrane proteins are poorly understood. Major advances have recently been made in the development of exogenous agents that can recognize these domains, which have laid the groundwork for targeting protein–protein interactions in the membrane bilayers (see picture).

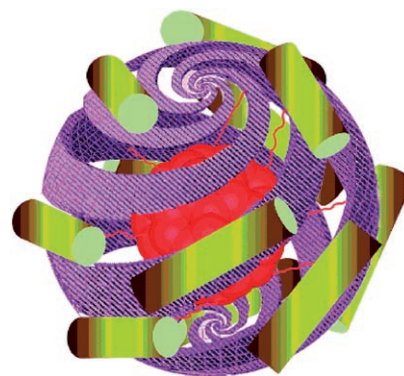
Reviews

Liquid Crystals

J. W. Goodby,* I. M. Saez, S. J. Cowling, V. Görtz, M. Draper, A. W. Hall, S. Sia, G. Cosquer, S.-E. Lee, E. P. Raynes _____ 2754–2787

Transmission and Amplification of Information and Properties in Nanostructured Liquid Crystals

Tune in your crystal set: Design of molecular shape, deformable molecular topologies, self-assembly, and self-organization combine together to yield super- and supramolecular liquid crystals (such as the nanomolecular “Boojum” shown in the picture) that are capable of exhibiting “superphases”. Transmission and amplification of physical properties are often observed for such systems.



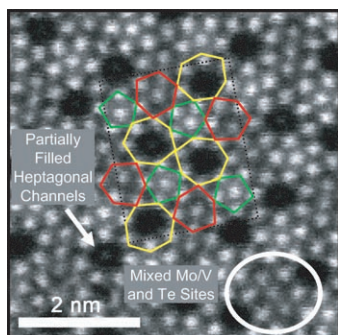
For the USA and Canada:

ANGEWANDTE CHEMIE International Edition (ISSN 1433-7851) is published weekly by Wiley-VCH, PO Box 191161, 69451 Weinheim, Germany. Air freight and mailing in the USA by Publications Expediting Inc., 200

Meacham Ave., Elmont, NY 11003. Periodicals postage paid at Jamaica, NY 11431. US POSTMASTER: send address changes to *Angewandte Chemie*, Wiley-VCH, 111 River Street, Hoboken, NJ 07030. Annual subscription price for institutions: US\$ 7225/6568 (valid for print and

electronic / print or electronic delivery); for individuals who are personal members of a national chemical society prices are available on request. Postage and handling charges included. All prices are subject to local VAT/sales tax.

Communications



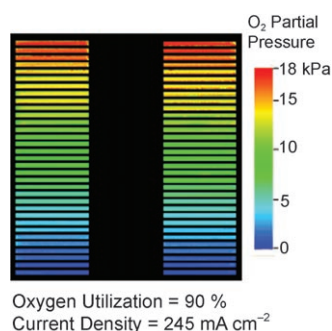
Seeing is believing: Aberration-corrected STEM imaging allows direct visualization of the orthorhombic M1 phase primary component of the MoVNbTeO propane ammoxidation catalyst. Atomic coordinates and site occupancies are obtained, and the beam-sensitive Te chains in the hexagonal and heptagonal channels are successfully imaged. These results suggest that HR-HAADF imaging may provide improved starting models for Rietveld analysis of complex structures.

STEM Imaging



W. D. Pyrz, D. A. Blom, T. Vogt,
D. J. Buttrey* — 2788 – 2791

Direct Imaging of the MoVTenbO M1 Phase Using An Aberration-Corrected High-Resolution Scanning Transmission Electron Microscope

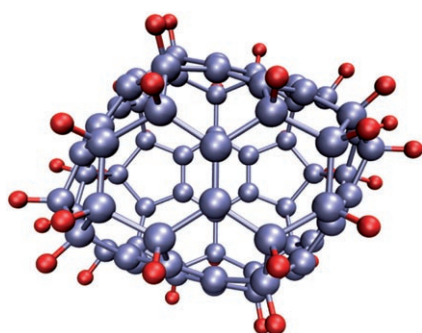


Cell diagnosis: The oxygen distribution in the interior of operating fuel cells can be visualized by using dye films painted on the transparent gas flow field (see image). The spatial and time resolutions are 300 μm and 500 ms, respectively. The oxygen distribution in a polymer electrolyte membrane fuel cell was not in accordance with that expected from the current, suggesting a significant contribution from water.

Fuel Cell Analysis

J. Inukai, K. Miyatake, K. Takada,
M. Watanabe,* T. Hyakutake, H. Nishide,
Y. Nagumo, M. Watanabe, M. Aoki,
H. Takano — 2792 – 2795

Direct Visualization of Oxygen Distribution in Operating Fuel Cells

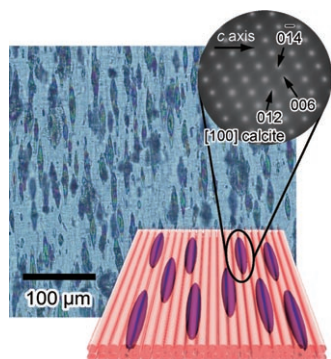


Feeling the pressure: Hydrogenation of C_{70} at 100 bar H_2 pressure and 400 °C for 72 h has enabled isolation of $\text{C}_{70}\text{H}_{38}$. Full structural assignment was achieved by 2D NMR spectroscopic studies, which show $\text{C}_{70}\text{H}_{38}$ to have C_2 symmetry and contain five benzenoid rings and two protonated carbon atoms on the equator (see picture). The proposed protonation scheme for the formation of this isomer shows a high similarity to reported $\text{C}_{70}\text{F}_{38}$ isomers.

Fullerenes

T. Wägberg, M. Hedenström, A. V. Talyzin,
I. Sethson, Y. O. Tsybin, J. M. Purcell,
A. G. Marshall, D. Noréus,
D. Johnels* — 2796 – 2799

Synthesis and Structural Characterization of $\text{C}_{70}\text{H}_{38}$



Unidirectionally aligned hybrids consisting of chitin and calcite were obtained by template crystallization of CaCO_3 in an ordered chitin film with nematic liquid-crystalline molecular alignment. The picture shows the resulting chitin matrix containing CaCO_3 rods, schematically and in the form of an optical micrograph, and the selected-area electron diffraction pattern of a thin section of a single rod.

Self-Organized Hybrids

T. Nishimura, T. Ito, Y. Yamamoto,
M. Yoshio, T. Kato* — 2800 – 2803

Macroscopically Ordered Polymer/ CaCO_3 Hybrids Prepared by Using a Liquid-Crystalline Template



Incredibly international!



386409711_st



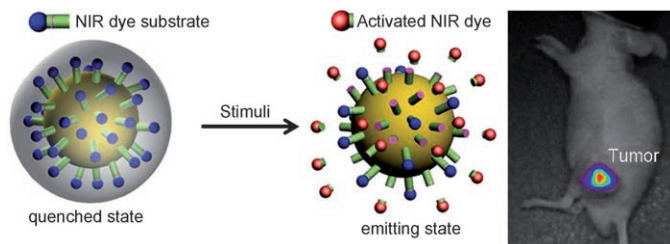
Although *Angewandte Chemie* is owned by the German Chemical Society (Gesellschaft Deutscher Chemiker, GDCh) and is published by Wiley-VCH in a charming small town in southwest Germany, it is international in every other respect. Authors and referees from around the globe contribute to its success. Most of the articles are submitted from China (20%), USA (16%), and Japan (13%) - only then comes Germany (12%). Most of the referee reports come from Germany and the USA, but Japan and Western Europe are also well represented.

service@wiley-vch.de
www.angewandte.org



GESELLSCHAFT
DEUTSCHER CHEMIKER





Nanodiagnosis: A matrix-metalloproteinase (MMP) sensitive gold-nanoparticle (AuNP) imaging probe quenches conjugated near-infrared (NIR) dyes with high efficiency and is specifically activated by the target MMPs (see picture, left). With

this system, nanomolar amounts of protease can be detected—both in vitro and in vivo. Experiments disclose an apparent positive contrast in MMPs-positive tumor-bearing mice (right).

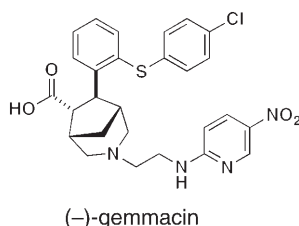
Gold Nanoprobes

S. Lee, E.-J. Cha, K. Park, S.-Y. Lee, J.-K. Hong, I.-C. Sun, S. Y. Kim, K. Choi, I. C. Kwon, K. Kim,*
C.-H. Ahn* ————— 2804–2807

A Near-Infrared-Fluorescence-Quenched Gold-Nanoparticle Imaging Probe for In Vivo Drug Screening and Protease Activity Determination



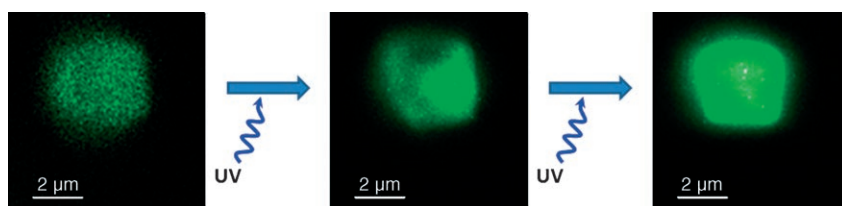
Beating the superbugs: Diversity-oriented synthesis using a solid-supported phosphonate unit to synthesize 242 drug-like compounds based on 18 natural-product-like scaffolds led to the discovery of gemmacin (see scheme). This new structural class of antibiotic is active towards methicillin-resistant *Staphylococcus aureus* (MRSA).



Combinatorial Chemistry

G. L. Thomas, R. J. Spandl, F. G. Glansdorp, M. Welch, A. Bender, J. Cockfield, J. A. Lindsay, C. Bryant, D. F. J. Brown, O. Loiseleur, H. Rudyk, M. Ladlow, D. R. Spring* — 2808–2812

Anti-MRSA Agent Discovery Using Diversity-Oriented Synthesis



The right bright light: Silver-exchanged zeolite 3A crystals show remarkable luminescent properties. Upon irradiation with high-power UV light, a strong photoactivation process takes place which results in

an emission increase of up to two orders of magnitude (see picture). The crystals of interest—or even small domains within one crystal—can be selectively activated by using a confocal microscope.

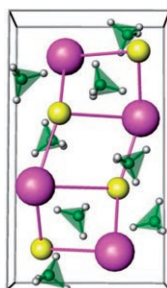
Silver in Zeolites

G. De Cremer, Y. Antoku, M. B. J. Roeffaers, M. Sliwa, J. Van Noyen, S. Smout, J. Hofkens, D. E. De Vos, B. F. Sels, T. Vosch* — 2813–2816

Photoactivation of Silver-Exchanged Zeolite A



Variegated decomposers: The synthesis of the first mixed alkali metal borohydride, which contains lithium and potassium, is presented. $\text{LiK}(\text{BH}_4)_2$ (see picture; K crimson, Li yellow, B green, H gray) has a crystal structure similar to LiBH_4 , and a thermal decomposition temperature between those of LiBH_4 and KBH_4 . Using this route, the hydrogen desorption thermodynamics of complex hydrides can be easily tailored.



Hydrogen Storage

E. A. Nickels, M. O. Jones, W. I. F. David,* S. R. Johnson, R. L. Lowton, M. Sommariva,
P. P. Edwards* ————— 2817–2819

Tuning the Decomposition Temperature in Complex Hydrides: Synthesis of a Mixed Alkali Metal Borohydride



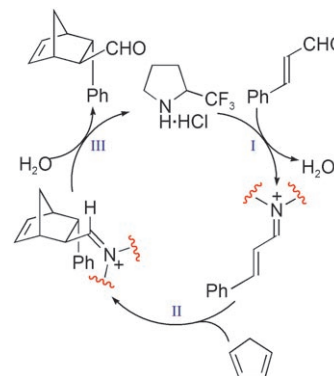
Organocatalysis

G. Evans, T. J. K. Gibbs, R. L. Jenkins,
S. J. Coles, M. B. Hursthouse, J. A. Platts,*
N. C. O. Tomkinson* — 2820–2823



Kinetics of Iminium Ion Catalysis

Identifying the bottleneck: Kinetic and computational data for the key steps of the iminium ion catalyzed Diels–Alder reaction show that the cycloaddition (step II in scheme) is the rate-determining step of the catalytic cycle and provide a rationale for developing more-active catalyst architectures.

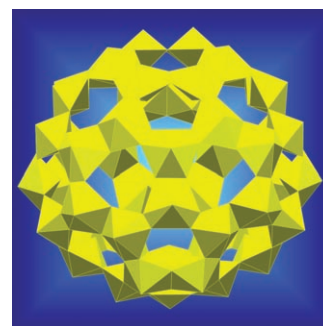


Inorganic Fullerene Structures

T. Z. Forbes, J. G. McAlpin, R. Murphy,
P. C. Burns* — 2824–2827

Metal–Oxygen Isopolyhedra Assembled
into Fullerene Topologies

Conditions that permit the assembly of metal–oxygen isopolyhedra into fullerene topologies favor the hexagonal bipyramid as the basic building unit. Uranyl hexagonal bipyramids containing two peroxide edges have been used to create a cage cluster with a fullerene topology containing 50 polyhedra (see picture), as well as cage cluster of 40 polyhedra that contains topological squares, pentagons, and hexagons.

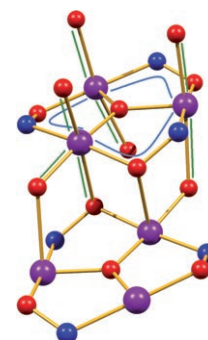


Pressure Effects

A. Prescimone, C. J. Milios, S. Moggach,
J. E. Warren, A. R. Lennie,
J. Sanchez-Benitez, K. Kamenev,
R. Bircher, M. Murrie, S. Parsons,*
E. K. Brechin* — 2828–2831

[Mn₆] under Pressure: A Combined
Crystallographic and Magnetic Study

Folding under pressure: High-pressure crystallography of an Mn₆ single-molecule magnet reveals dramatic changes in the intramolecular geometry of the magnetic core (see picture; Mn purple, O red, N blue). These structural changes effect the magnetic properties of the molecule: the magnitude of the ferromagnetic exchange between the metals is decreased, and under extreme pressure switches to anti-ferromagnetic.

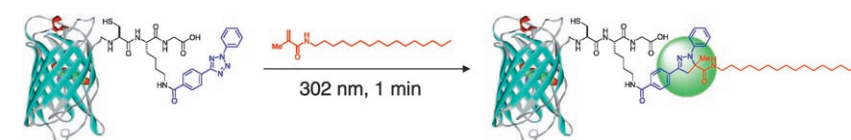


Bioorthogonal Chemistry

W. Song, Y. Wang, J. Qu, M. M. Madden,
Q. Lin* — 2832–2835

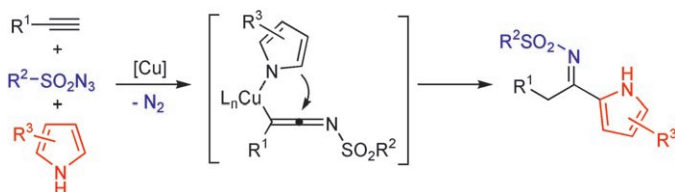


A Photoinducible 1,3-Dipolar
Cycloaddition Reaction for Rapid,
Selective Modification of Tetrazole-
Containing Proteins



Reactive but biologically inert: The bioorthogonal title reaction enables highly specific chemical modifications, such as lipidation, of engineered proteins containing a diphenyltetrazole group (see

scheme). The cycloaddition in biological media is extremely fast (≤ 1 min) and tolerant of proteinaceous groups. Strongly fluorescent pyrazoline cycloadducts are generated with simple alkenes.



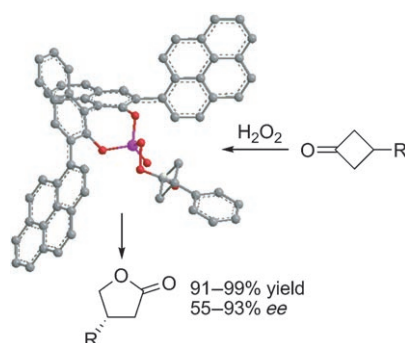
Making rings: A new Cu-catalyzed three-component coupling reaction between 1-alkynes, sulfonamides, and pyrrole derivatives has been developed for making 2-functionalized pyrrole rings (see

scheme). This C–C bond formation offers high efficiency and selectivity, mild reaction conditions, and a wide substrate scope.

Pyrrole Functionalization

S. H. Cho, S. Chang* — 2836–2839

Room Temperature Copper-Catalyzed 2-Functionalization of Pyrrole Rings by a Three-Component Coupling Reaction



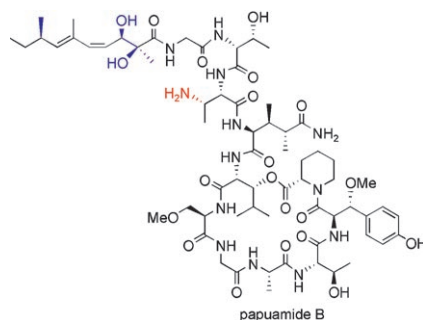
A catalytic amount of a chiral Brønsted acid with aqueous H₂O₂ as the oxidant is sufficient for the enantioselective Baeyer–Villiger oxidation of 3-substituted cyclobutanones to give the corresponding γ -lactones in excellent yields and up to 93% ee. The method employs benign aqueous H₂O₂ instead of stoichiometric amounts of a dangerous peracid.

Asymmetric Catalysis

S. Xu, Z. Wang, X. Zhang, X. Zhang, K. Ding* — 2840–2843

Chiral Brønsted Acid Catalyzed Asymmetric Baeyer–Villiger Reaction of 3-Substituted Cyclobutanones by Using Aqueous H₂O₂

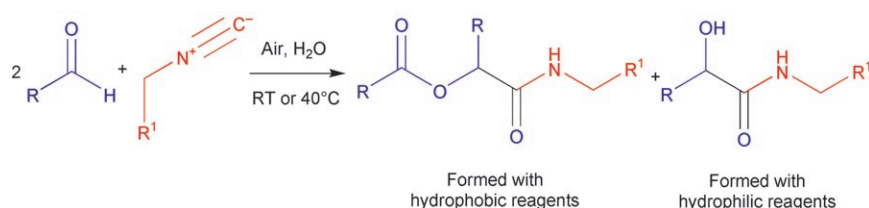
Synthesis in stereo: The first total synthesis of papuamide B, a cyclic peptide isolated from a marine sponge, has been achieved. The configuration of three stereogenic centers of its dienoic acid unit has been established by comparison to a series of stereoisomers of known configuration, and the stereochemistry of its 2,3-diaminobutanoic acid segment has been revised.



Natural Product Synthesis

W. Xie, D. Ding, W. Zi, G. Li, D. Ma* — 2844–2848

Total Synthesis and Structure Assignment of Papuamide B, A Potent Marine Cyclodepsipeptide with Anti-HIV Properties



Wet, wet, wet: Hydrophobic aldehydes are cleanly oxidized upon stirring with water in air. Addition of hydrophobic isocyanides to aqueous suspensions of such aldehydes results in the formation of Passerini reaction products, with the

aldehyde being the source of both carbonyl and ester functions. Partially water-soluble reagents reacted slower than water-insoluble ones. Isotope labeling studies show that water participates in these “on water” reactions.

Organic Synthesis

N. Shapiro, A. Vigalok* — 2849–2852

Highly Efficient Organic Reactions “on Water”, “in Water”, and Both

Functional Foldamers

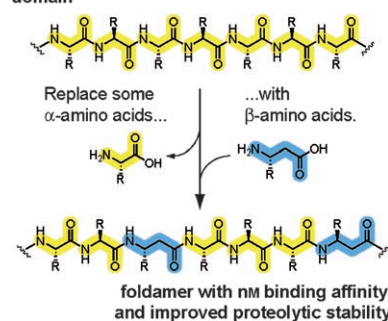
W. S. Horne, M. D. Boersma,
M. A. Windsor,
S. H. Gellman* — 2853–2856



Sequence-Based Design of α/β -Peptide Foldamers That Mimic BH3 Domains

Into the fold: Foldamers have emerged as versatile scaffolds for the design of functional macromolecules. A straightforward design principle based on primary sequence can be used to convert an α -peptide ligand derived from a natural protein-binding domain into an α/β -peptide with comparable binding affinity for protein targets bound by the α -peptide (see scheme).

natural protein-binding domain

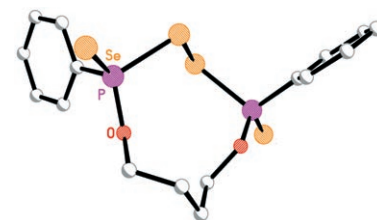


Organic P–Se Rings

G. Hua, Y. Li, A. M. Z. Slawin,
J. D. Woollins* — 2857–2859

Synthesis and Structure of Eight-, Nine-, and Ten-Membered Rings with P–Se–Se–P Linkages

Full circle: The reaction of $[\text{PhP}(\text{Se})(\mu\text{-Se})_2]$ with alkyl or aryl diols affords five unusual P–Se heterocycles with eight-, nine-, and ten-membered rings containing P–Se–Se–P linkages. The structure of the ten-membered ring is shown.

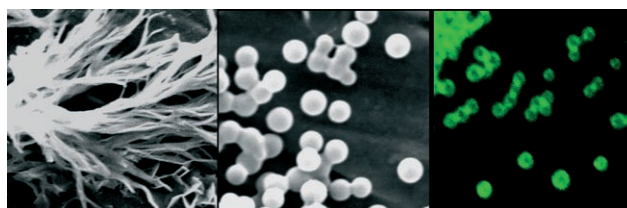


Biotin Structures

K. B. Joshi, S. Verma* — 2860–2863



Di-tryptophan Conjugation Triggers Conversion of Biotin Fibers into Soft Spherical Structures



Trigger happy: Biotin and its methyl ester form long fibers in solution, which are transformed into soft spherical structures upon simple conjugation with di-tryptophan

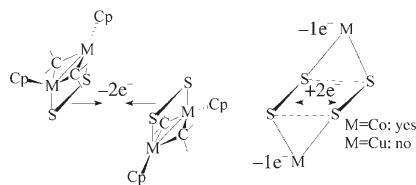
phan dipeptide (see picture). Such morphogenesis is not achieved in a controlled fashion by other aromatic amino acids.

Electronic Structure

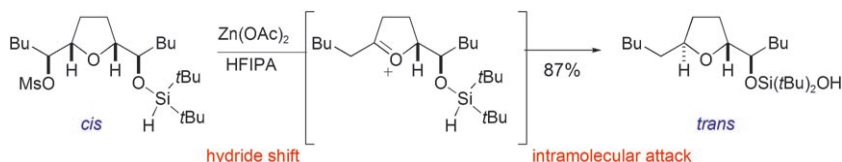
C. Mealli,* A. Ienco, A. Poduska,
R. Hoffmann* — 2864–2868



S_4^{2-} Rings, Disulfides, and Sulfides in Transition-Metal Complexes: The Subtle Interplay of Oxidation and Structure



Coming together, breaking apart: A theoretical analysis of the oxidative coupling of two metal-coordinated disulfide species to a S_4^{2-} rectangle provides an opening to a reexamination of a number of compounds hitherto considered to be disulfide complexes. An electronic framework helps explain how the nature of the metal controls inner redox processes and the alternative stabilization of S_4^{2-} or 2S_2^{2-} (or S^{2-}) species (see scheme).



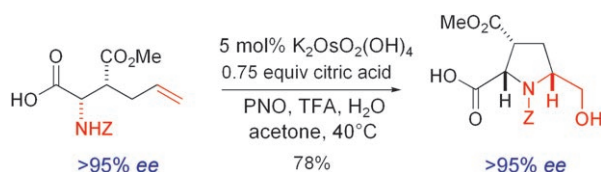
Switching sides: *cis* THF derivatives produced from the oxidative cyclization of dienes and diols can be transformed into the corresponding *trans* heterocycles through a 1,2-hydride shift and intramolecular trapping with a hydride nucleo-

phile (see scheme). Moreover, organometallic compounds can be used to trap the oxonium ion generated in this way so that it is possible to introduce various groups at the C-2 position with control of stereochemistry.

Stereoselective Synthesis

T. J. Donohoe,* O. Williams,
G. H. Churchill — 2869–2871

Hydride Shift Generated Oxonium Ions:
Evidence for Mechanism and
Intramolecular Trapping Experiments to
Form *trans* THF Derivatives



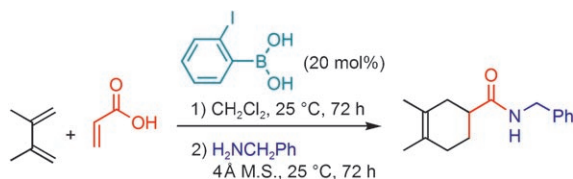
The PNOman can: The use of pyridine-*N*-oxide (PNO) transforms the catalytic oxidative cyclization to include the formation of pyrrolidines from *N*-*Z*-protected amino alcohols and amino acids (see scheme; *Z* = PhCH₂OCO). This new

method expands the scope of the oxidative cyclization as illustrated with the synthesis of a range of di- and trisubstituted pyrrolidines with complete control of stereochemistry.

Oxidative cyclization

T. J. Donohoe,*
K. M. P. Wheelhouse (née Gosby),
P. J. Lindsay-Scott, P. A. Glossop,
I. A. Nash, J. S. Parker — 2872–2875

Pyridine-*N*-Oxide as a Mild Reoxidant
Which Transforms Osmium-Catalyzed
Oxidative Cyclization



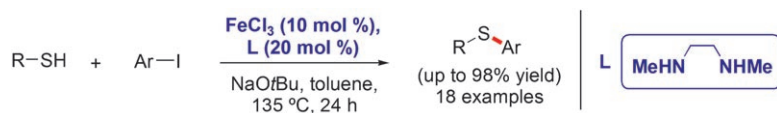
Taming carboxylic acids: *ortho*-Iodo- and *ortho*-bromophenylboronic acids are exceptional organocatalysts in atom-economical amidations between free carboxylic acids and amines, including func-

tionalized ones, and can also provide LUMO-lowering activation in [4+2] cycloadditions of α,β -unsaturated carboxylic acids.

Organocatalysis

R. M. Al-Zoubi, O. Marion,
D. G. Hall* — 2876–2879

Direct and Waste-Free Amidations and
Cycloadditions by Organocatalytic
Activation of Carboxylic Acids at Room
Temperature



Strike while the iron is hot: An efficient iron-catalyzed protocol for the S-arylation of aromatic and heteroaromatic thiol derivatives has been developed, which involves an inexpensive catalyst system formed by combining FeCl₃ and *N,N'*-

dimethylethylenediamine at 135°C. This method avoids the use of expensive and/or air-sensitive ligands and provides in most cases the desired sulfide in high yields.

Cross-Coupling Reactions

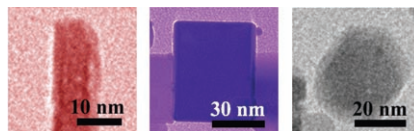
A. Correa, M. Carril,
C. Bolm* — 2880–2883

Iron-Catalyzed S-Arylation of Thiols with
Aryl Iodides



Shape effects

R. Si, M. Flytzani-Stephanopoulos* _____ 2884–2887



A two-step synthesis method is used to prepare gold-on-ceria nanorods, nanocubes, and nanopolyhedra (see picture), and a strong shape-effect of CeO_2 on the water–gas shift reaction activity of the catalysts is identified. Gold on the (110) facets of ceria nanorods shows the highest activity.



Shape and Crystal-Plane Effects of Nanoscale Ceria on the Activity of Au- CeO_2 Catalysts for the Water–Gas Shift Reaction



Supporting information is available on www.angewandte.org (see article for access details).



A video clip is available as Supporting Information on www.angewandte.org (see article for access details).

Looking for outstanding employees?

Do you need another expert for your excellent team?
... Chemists, PhD Students, Managers, Professors, Sales Representatives...

Place an advert in the printed version and have it made available online for 1 month, free of charge!

Angewandte Chemie International Edition

Advertising Sales Department: Marion Schulz

Phone: 0 62 01 - 60 65 65

Fax: 0 62 01 - 60 65 50

E-Mail: MSchulz@wiley-vch.de

Service

Spotlights Angewandte's
Sister Journals _____ 2724–2725

Keywords _____ 2888

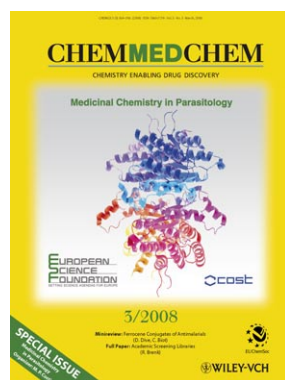
Authors _____ 2889

Preview _____ 2891

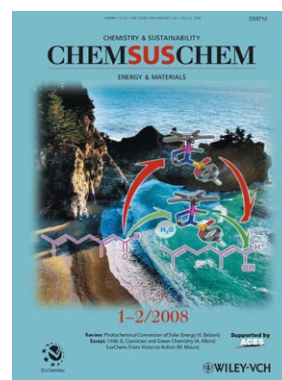
For more Information see:



www.chemasianj.org



www.chemmedchem.org



www.chemsuschem.org